Kinetics and Catalysis, Vol. 43, No. 4, 2002, pp. 495–506. Translated from Kinetika i Kataliz, Vol. 43, No. 4, 2002, pp. 538–549.
Original Russian Text Copyright © 2002 by Radtsig.

Kinetics of Intramolecular Hydrogen Atom Transfer in the Radicals $>\mathrm{Si}(\mathrm{O}^{\bullet})(\mathrm{R})$ (R = H, D, CH_3, CD_3, and C_2H_5)

V. A. Radtsig

Semenov Institute of Chemical Physics, Russian Academy of Sciences, Moscow, 117977 Russia

Received January 15, 2002

Abstract—Methods are developed for obtaining oxy radicals by the photodecomposition and thermal decomposition of precursors $(\equiv\mathrm{Si{-}O})_2\mathrm{Si(N{=}N{-}O^{\bullet})(R)}$ and $(\equiv\mathrm{Si{-}O})_2\mathrm{Si(O{-}C^{\bullet}{=}O)(R)}$. The mechanism of these processes is established. Kinetic data are obtained for the reaction of hydrogen atom transfer in oxy radicals $(\equiv\mathrm{Si{-}O})_2\mathrm{Si(O^{\bullet})(R)}$ (R = H, D, CH_3, CD_3, and C_2H_5). The activation energies of hydrogen atom transfer are found for three-, four-, and five-membered transition states: 13.5 ± 1, 18 ± 1, and <10 kcal/mol, respectively. For the reaction of H(D) atom transfer in the $(\equiv\mathrm{Si{-}O})_2\mathrm{Si(O^{\bullet})(H(D))}$ radical, the kinetic isotope effect is found. Quantum-chemical calculations were used to determine the structures of transition states in the studied processes. Experimental studies were carried out using ESR spectroscopy.

INTRODUCTION

Although tremendous experimental and theoretical work has been devoted to the structure and reactivity of chemically active species, interest in this field does not fade. This is due to an important role of these species in various processes in the gas and condensed phases. However, most of the experimental data obtained so far refer to bimolecular processes of reactive species, such as hydrogen atom abstraction or the interactions of free radicals with other radicals available in a system. Unimolecular reactions, such as isomerization and decomposition of free radicals, received less attention. The experimental studies of such processes are more difficult because of the following circumstances. Processes with the participation of free radicals are usually studied in either gas or condensed phases, where unimolecular reactions are masked by bimolecular reactions of radicals with ambient molecules and with each other. Such bimolecular reactions are usually much faster. The use of the matrix isolation technique enables the stabilization of radicals, but these matrices are thermally unstable. Therefore, these systems cannot be used for the studies of thermal processes with activation energies of several kcal/mol.

A new method has been proposed in [1–3] for obtaining free radical intermediates grafted on a solid surface (reactive silica). In this work, we applied this method to experimentally study the mechanism and kinetics of the reactions of intramolecular H(D) atom transfer in oxysilyl radicals $>\mathrm{Si(O^{\bullet})(R)}$, where R = H, D, CH_3, CD, and C_2H_5. Oxy radicals of the silicon type belong to the most reactive species. Specifically, the activation energy of the reaction of H(D) atom abstraction from unsaturated hydrocarbons with the participation of these radicals is close to zero [4]. However, in this case, reactions of H(D) atom transfer occur via the cyclic transition state. Thus, these systems are convenient for the study of the size effect of cyclic transition states on the activation energies of reactions.

EXPERIMENTAL

The method of preparation and activation of the surfaces of highly dispersed silica was described in detail in the preceding paper [5]. Intermediates with the desired structure were obtained in two stages. First, silyl-type radicals were obtained using silylene centers $(\equiv\mathrm{Si{-}O})_2\mathrm{Si}$: (henceforth denoted as $>\mathrm{Si}$:), which are stabilized on the surface of reactive silica [6, 7], and low-molecular radicals $\mathrm{R}^{\bullet}$:

$$>\mathrm{Si}: + \mathrm{R}^{\bullet} \longrightarrow >\mathrm{Si}^{\bullet}\mathrm{R}. \tag{I}$$

Low-molecular radicals used in this work were $\mathrm{H}^{\bullet}$, $\mathrm{D}^{\bullet}$, ${}^{\bullet}\mathrm{CH}_3$, ${}^{\bullet}\mathrm{CD}_3$, and ${}^{\bullet}\mathrm{C_2H_5}$. They were obtained from the H_2, D_2, CH_4, CD_4, and C_2H_6 molecules using either surface oxy radicals $(\equiv\mathrm{Si{-}O})_3\mathrm{Si{-}O^{\bullet}}$ [4],

$$(\equiv\mathrm{Si{-}O})_3\mathrm{Si{-}O^{\bullet}} + \mathrm{R{-}H(D)}$$

$$\longrightarrow (\equiv\mathrm{Si{-}O})_3\mathrm{Si{-}O{-}H(D)} + \mathrm{R}^{\bullet},$$

as radical generators or surface diamagnetic groups $>\mathrm{Si}<\mathrm{O}_2$ [8]:

$$>\mathrm{Si}<\mathrm{O}_2 + \mathrm{R{-}H(D)} \longrightarrow\, >\mathrm{Si(O^{\bullet})(O{-}H(D))} + \mathrm{R}^{\bullet},$$

$$>\mathrm{Si(O^{\bullet})(O{-}H(D))} + \mathrm{R{-}H(D)}$$

$$\longrightarrow\, >\mathrm{Si(O{-}H(D))(O{-}H(D))} + \mathrm{R}^{\bullet}.$$

For more details, see [9].

Then, the $>\mathrm{Si}^{\bullet}\mathrm{R}$ radicals entered a reaction with $\mathrm{N_2O}$ or $\mathrm{CO_2}$ molecules at room temperature [10, 11]:

$$>\mathrm{Si}^{\bullet}\mathrm{R} + \mathrm{N_2O} \longrightarrow\, >\mathrm{Si(N{=}N{-}O^{\bullet})(R)},$$

$$>\mathrm{Si}^{\bullet}\mathrm{R} + \mathrm{CO_2} \longrightarrow\, >\mathrm{Si(O{-}C^{\bullet}{=}O)(R)}$$

to obtain the desired free radical complexes.

These two types of paramagnetic complexes served as precursors of oxy radicals. The reactions of their thermal decomposition occurred as follows (see [11] and subsection 2 of this paper):

$$>\mathrm{Si(N{=}N{-}O^{\bullet})(R)} \longrightarrow\, >\mathrm{Si(O^{\bullet})(R)} + \mathrm{N_2}, \qquad \text{(II)}$$

$$>\mathrm{Si}^{\bullet}\mathrm{R} + \mathrm{CO_2} \rightleftarrows\, >\mathrm{Si(O{-}C^{\bullet}{=}O)(R)} \qquad \text{(III)}$$

$$\rightleftarrows\, >\mathrm{Si(O^{\bullet})(R)} + \mathrm{CO}.$$

However, these reactions occur with measurable rates only at high temperatures (≥373 K). Under these conditions, the transfer of a hydrogen atom to oxygen in group R occurs at a much higher rate than the rate of oxy radical formation (see below). Therefore, we can only obtain the lower estimate of the rate constant of H(D) transfer to the oxygen atom in this case.

One of the ways to overcome this difficulty is to use the method of competing reactions. For instance, if the process of thermal decomposition of the precursor is carried out in a CO atmosphere (reaction (III)), then an alternative channel for the transformation of the oxy radical appears, which is associated with the reverse addition of the CO molecule and results in the reduction of the silyl-type radical. By measuring the ratio of product yields in these two channels at different CO pressures, we can determine the ratio of the rate constants of these two competing processes.

Oxysilyl radicals can also be obtained by the photochemical decomposition of $>\mathrm{Si(N{=}N{-}O^{\bullet})(R)}$ precursors [11]. Photolysis can also be carried out at low temperatures (77 K). Provided that oxy radicals remain stable at low temperatures, the direct spectroscopic studies of further thermal transformations in these systems become possible. Spectroscopy was applied to study H(D) atom transfer in the radicals $>\mathrm{Si(O^{\bullet})(R)}$ (R = H(D) and $\mathrm{CH_3(CD_3)}$).

ESR spectra of radicals were recorded using an EPR-20 radiospectrometer working in an X-range (a frequency of 9.1 MHz). The frequency of high-frequency modulation was 100 kHz. The magnetizing force was registered using an NMR magnetometer. The radiospectrometer was connected to a PC through an interface. At 77 K, the ESR spectra were registered by putting the sample into a quartz Dewar bottle filled with liquid nitrogen. The constant temperature of the sample in the resonator was maintained by a flow of gaseous nitrogen.

Photolysis of samples was carried out using a DRSh-1000 high-pressure mercury lamp equipped with a water filter, which transmits radiation with $E <$ 5.2 eV and cuts off the infrared part of the spectrum of lamp radiation, and with standard light filters. The sample was irradiated with the filtered (light filter FS-1) light of the mercury lamp. Photolysis at 77 K was carried out in a Dewar bottle filled with liquid nitrogen.

IR spectroscopic measurements were carried out for the samples that were made of pressed highly dispersed Aerosil semitransparent films (50–100-μm thick) [12], placed in a special cell with silica windows. For these samples, one can register IR spectra at wavenumbers in the region of ≥1300 $\mathrm{cm^{-1}}$. IR spectra were recorded at room temperature using a Digilab Fourier-transform spectrometer with 4-$\mathrm{cm^{-1}}$ resolution and 256 scans.

Quantum-chemical calculations were carried out using Gaussian-94 [13]. The structures of molecules, radicals, and transition states for different channels of their transformation were optimized by minimizing the gradient norm. For all optimized structures, vibrational spectra were simulated. Each transition state had one negative eigenvalue of the Hessian matrix.

RESULTS AND DISCUSSION

1. Generation of Oxy Radicals in the $>\mathrm{Si(N{=}N{-}O^{\bullet})(R)}$ Systems by the Photochemical Method

1.1. Photolysis of $>\mathrm{Si(N{=}N{-}O^{\bullet})(CH_3(CD_3))}$ radicals. Optical absorption spectrum of $>\mathrm{Si(N{=}N{-}O^{\bullet})(R)}$ radicals consists of three bands with maxima at 3.25, 5.2, and >6 eV [11]. Irradiation with light in the region of the long-wave absorption band of radicals (using an FS-1 light filter) results in photodecomposition [11]. Figure 1a shows changes in the ESR spectrum of a sample containing radicals $>\mathrm{Si(N{=}N{-}O^{\bullet})(CH_3)}$ after its irradiation for 30 min at 77 K (to prevent sample heating in the process of photolysis, an ampule with powder was filled with helium (0.5 torr)). A decrease in the intensity of the lines of initial radical by a factor of ~2 is accompanied by the appearance of a characteristic ESR spectrum of the $>\mathrm{Si}^{\bullet}{-}\mathrm{CH_3}$ radical in the center [8]. This spectrum, which is shown separately in Fig. 1b, was registered at a decreased level of microwave power

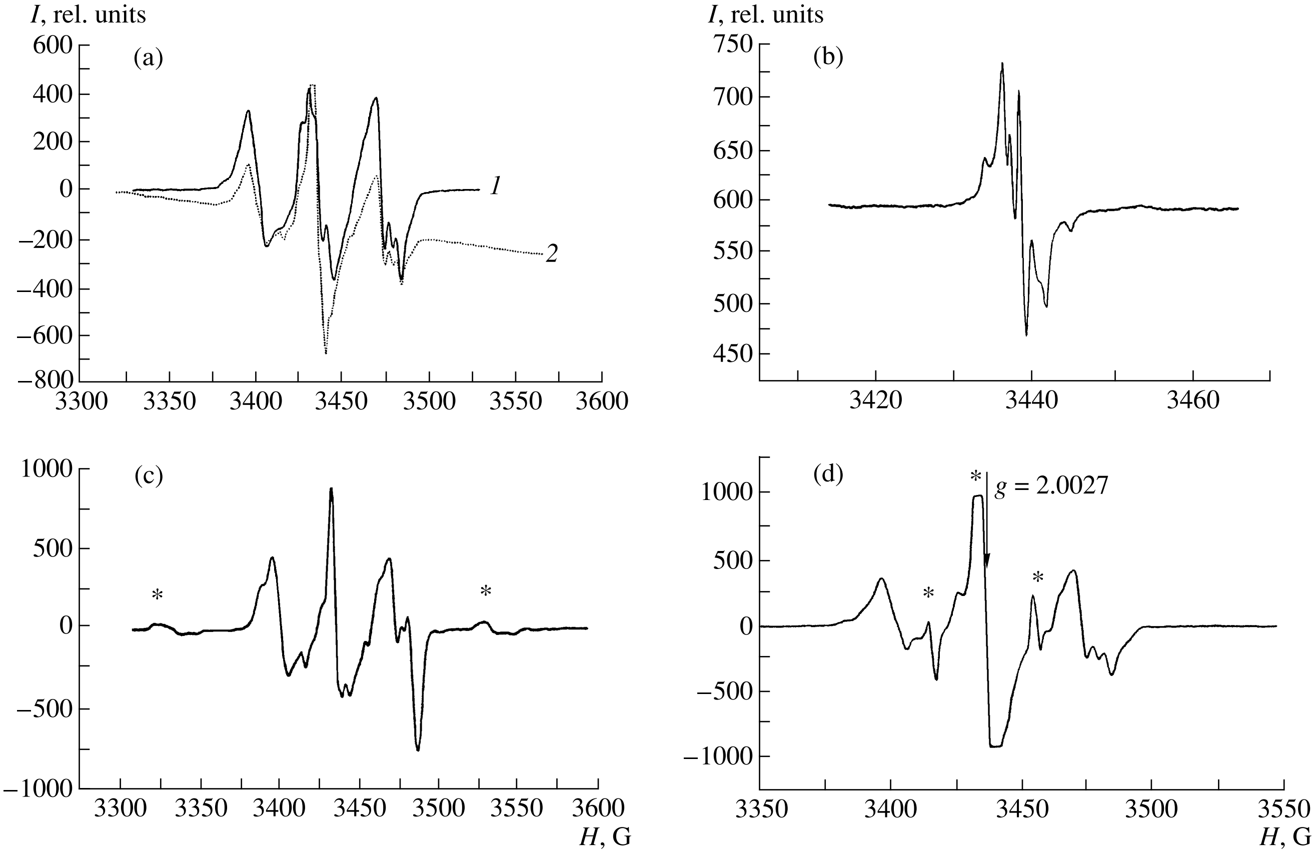

Fig. 1. ESR spectra of radicals $>$Si(N=N–O$^\bullet$)(CH$_3$) and products of their photolysis: (a) (*1*) before photolysis and (*2*) after photolysis of the sample at 77 K; (b) the central part of spectrum *2* registered at a low level of microwave power; (c) the spectrum of sample 2 after its treatment by ^{13}CO molecules at 77 K (two lines marked with stars refer to the $>$Si(O–^{13}C$^\bullet$=O)(CH$_3$) radical; and (d) sample 2 heated at 250 K (lines marked with stars refer to the $>$Si(OH)($\text{CH}_2^\bullet$) radicals. Recording at 77 K.

(this signal saturates at the level of microwave power at which the spectrum shown in Fig. 1a was registered).

Photolysis also yielded oxy radicals. Their direct registration by ESR spectroscopy is hampered due to the specific features of their electronic structure [2]. For their detection using the ESR method, we used the following expedient. The sample was treated with ^{13}CO molecules without preliminary heating (i.e., at 77 K). It is known that oxy radials react with carbon monoxide molecules even at 77 K [10]:

$$>\text{Si–O}^\bullet(\text{R}) + {}^{13}\text{CO} \longrightarrow >\text{Si(O–}{}^{13}\text{C}^\bullet\text{=O)(R)}.$$

Figure 1c shows the ESR spectrum of the product of this reaction. Stars mark lines corresponding to the splitting of the spectrum components on the ^{13}C nucleus ($I = 1/2$). The constant of hyperfine interaction of the unpaired electron with the ^{13}C nucleus was 208 Oe. This value is characteristic of the oxycarbonyl radials $>$Si(O–C$^\bullet$=O)(R) containing hydrocarbon substituent R at a silicon atom [8]. Thus, the photolysis of the radical at 77 K was accompanied by the formation of two main products of photodecomposition: silyl and oxysilyl radicals:

$$\begin{array}{c} >\text{Si(N=N–O}^\bullet)(\text{CH}_3) \longrightarrow >\text{Si}^\bullet(\text{CH}_3) + \text{N}_2\text{O} \\ \text{(channel 1),} \\ >\text{Si(N=N–O}^\bullet)(\text{CH}_3) \longrightarrow >\text{Si(O}^\bullet)(\text{CH}_3) + \text{N}_2 \\ \text{(channel 2).} \end{array} \qquad \text{(IV)}$$

The relative yields of these products are shown in Table 1. In another run, the sample subjected to photolysis under analogous conditions was heated from 77 to 350 K (5-min heating at a certain temperature with further registration of the ESR spectrum at 77 K). When the sample was heated to 180 K, the appearance of two lines was noticed in the ESR spectrum (they are marked with stars in Fig. 1e). These lines belong to the $>$Si(OH)($\text{CH}_2^\bullet$) radical. The ESR spectrum of this radical was registered and described in [14] and is also shown in Fig. 4c. Figure 2 (curve *1*) shows a change in the relative intensity in the sample heating to 350 K.

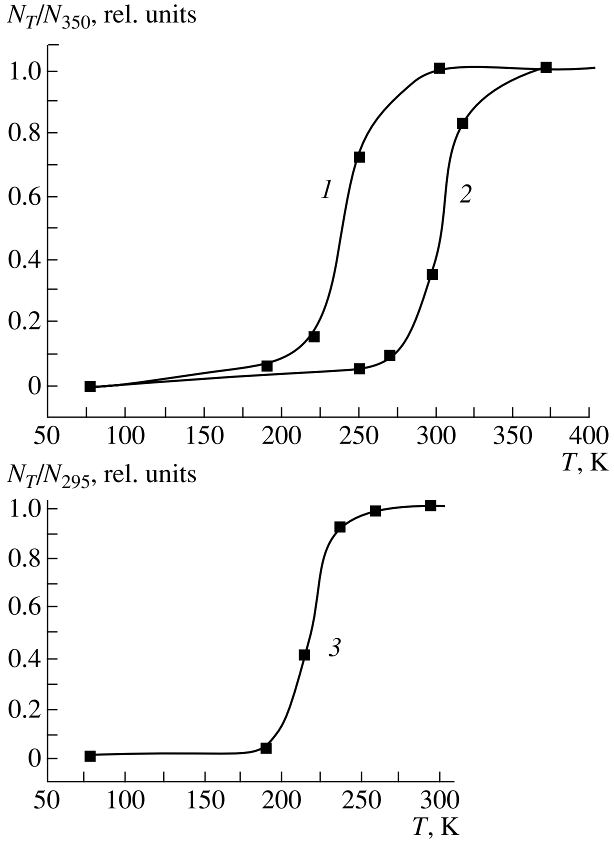

Fig. 2. Formation of products of oxy radical isomerization (*1*) $\mathrm{>Si(O^{\bullet})(CH_3)}$, (*2*) $\mathrm{>Si(O^{\bullet})(CD_3)}$, (*3*) $\mathrm{>Si(O^{\bullet})(D)}$, *1*—$\mathrm{>Si(OH)(CH_2^{\bullet})}$, *2*—$\mathrm{>Si(OD)(CD_2^{\bullet})}$, 3—$\mathrm{>Si^{\bullet}(OD)}$ on heating from 77 K. The units are relative: N_T/N_{350} (N_T/N_{295}), where N_T is the intensity of the ESR signal after sample heating at temperature T (5 min).

Thus, the above experimental data point to the fact that, in the process of photolysis, oxy radicals $\mathrm{>Si(O^{\bullet})(CH_3)}$, which are stable at low temperatures, are formed in the system. When the sample is heated in the temperature range 180–300 K, intramolecular hydrogen atom transfer occurs:

$$\mathrm{>Si(O^{\bullet})(CH_3)} \longrightarrow \mathrm{>Si(OH)(CH_2^{\bullet})}.$$

Table 1. Relative yields of photolysis products via channels 1 and 2 of reactions (IV)–(VI), $T = 77 \pm 1$ K

Radical	Via channel 1	Via channel 2
$\mathrm{>Si(N{=}N{-}O^{\bullet})(H)}$	0.61 ± 0.05	0.39 ± 0.05
$\mathrm{>Si(N{=}N{-}O^{\bullet})(D)}$	0.61 ± 0.05	0.39 ± 0.05
$\mathrm{>Si(N{=}N{-}O^{\bullet})(CH_3)}$	0.18 ± 0.05	0.82 ± 0.05
$\mathrm{>Si(N{=}N{-}O^{\bullet})(CD_3)}$	0.24 ± 0.05	0.76 ± 0.05

The activation energy estimated from kinetic data (Table 2) for this process is 16 (17) kcal/mol (the value of the preexponential factor is taken equal to 10^{12} (10^{13}) s^{-1}).

In another run, we prepared the deuterated radical $\mathrm{>Si(N{=}N{-}O^{\bullet})(CD_3)}$ (in which case we used deuterated methane instead of methane in radical synthesis). Photolysis of this sample was carried out under analogous conditions. A decrease in the concentration of the $\mathrm{>Si(N{=}N{-}O^{\bullet})(CD_3)}$ radical and the partial reduction of $\mathrm{>Si^{\bullet}(CD_3)}$ radicals was registered after photolysis (77 K) using the ESR method. Sample heating is accompanied by the formation of the $\mathrm{>Si(CD_2^{\bullet})(O{-}D)}$ radical. Thus, the process occurs in a similar manner in this system: the formation of two main photolysis products, $\mathrm{>Si^{\bullet}(CD_3)}$ and $\mathrm{>Si(O^{\bullet})(CD_3)}$ radicals, was found in this system, too. These radicals are stable at low temperatures and transform into the $\mathrm{>Si(CD_2^{\bullet})(O{-}D)}$ radicals on heating via the intramolecular transfer of the deuterium atom.

Figure 2 shows the dependence of the relative intensity of the ESR spectrum of radicals on the temperature of sample heating (curve *2*; ESR measurements; the time of heating at each temperature is 5 min). Thus, the isotopic substitution only affected the kinetics of H(D) atom transfer (see Table 2) and noticeably increased the temperature of the corresponding transformation. This fact points to the effect of isotopic substitution on the rate constant of this process. The value of the activation energy of deuterium transfer is 21.5 kcal/mol (this is estimated similarly as in the previous case).

In the classical case, the value of the isotope effect for the reactions of this type is due to the differences in the zero-point energies of the C–H and C–D bonds, whose H(D) atom participates in the process. For the processes of considered type, we could expect that this value is 1.5 kcal/mol [15]. The observed isotope effect was noticeably higher. To find the reasons for such a difference, detailed kinetic studies of these reactions at different temperatures are needed.

1.2. Photolysis of $\mathrm{>Si(N{=}N{-}O^{\bullet})(H(D))}$ radicals.

We begin this section with experimental data obtained for the $\mathrm{>Si(N{=}N{-}O^{\bullet})(D)}$ system. Figure 3a shows the ESR spectrum of sample photolysis at 77 K (the ESR spectra shown in this figure were registered under conditions when the signal from the much broader $\mathrm{>Si(N{=}N{-}O^{\bullet})(D)}$ radical with a much smaller amplitude is poorly discernible). On the edges of the spectra, two asymmetric lines of a triplet signal from the $\mathrm{>Si^{\bullet}(D)}$ radical are seen (the third component of this radical is in the middle of the signal). This is due to the interaction of an unpaired electron with deuteron

($I = 1$). Their positions are marked in the figure with stars.

Sample heating resulted in the appearance of new paramagnetic centers. The anisotropic line in the center of spectra (marked with a rhomb) belongs to them and is due to the $>\mathrm{Si}^{\bullet}(\mathrm{OD})$ radicals. The ESR spectrum of this radical was identified in [14]. The concentrations of two other radicals, $>\mathrm{Si}(\mathrm{N{=}N{-}O}^{\bullet})(\mathrm{D})$ and $>\mathrm{Si}^{\bullet}(\mathrm{D})$, which were present in the system, remained constant. The kinetic curve of $>\mathrm{Si}^{\bullet}(\mathrm{OD})$ formation in sample heating is shown in Fig. 2 (curve *3*).

Thus, two channels of phototransformations were detected in the photolysis of this system:

$$>\mathrm{Si}(\mathrm{N{=}N{-}O}^{\bullet})(\mathrm{D}) \longrightarrow >\mathrm{Si}^{\bullet}(\mathrm{D}) + \mathrm{N_2O} \text{ (channel 1)}, \tag{V}$$
$$>\mathrm{Si}(\mathrm{N{=}N{-}O}^{\bullet})(\mathrm{D}) \longrightarrow >\mathrm{Si}(\mathrm{O}^{\bullet})(\mathrm{D}) + \mathrm{N_2} \text{ (channel 2)}.$$

The relative yields of photolysis products are shown in Table 1.

The kinetics of $>\mathrm{Si}^{\bullet}{-}\mathrm{O{-}D}$ radical formation (Fig. 2, curve *3*) is typical of a thermally activated reaction. The rate constant of this reaction at 210 K is $k_2(\mathrm{D}) = 2 \times 10^{-3}\ \mathrm{s^{-1}}$ (see Table 2). This makes it possible to estimate the activation energy of deuterium atom transfer: ~15 kcal/mol (the preexponential factor is taken equal to $A_0 = 10^{13}\ \mathrm{s^{-1}}$).

Let us now proceed to the experimental data obtained in the study of processes with the H-form of this radical. The general picture of the phototransformation is preserved: the intensity of the lines of the initial radical decreases, and the intensities of the reaction product lines synchronously increase. However, an important difference appeared. Figure 3b shows the ESR spectrum of photolysis products at 77 K (registration at 77 K without intermediate sample heating). The lines of $>\mathrm{Si}^{\bullet}\mathrm{H}$ and $>\mathrm{Si}^{\bullet}\mathrm{OH}$ radicals are distinctly seen in the spectrum (these are marked with a rhomb and an asterisk, respectively). Sample heating to room temperature did not lead to a change in the concentrations of radicals in the system. Thus, the photochemical process in this system occurs as in the case of the $>\mathrm{Si}(\mathrm{N{=}N{-}O}^{\bullet})(\mathrm{D})$ radical via two channels: with the elimination of $\mathrm{N_2}$ and $\mathrm{N_2O}$ molecules, but the reaction of hydrogen atom transfer completes even at 77 K:

$$>\mathrm{Si}(\mathrm{N{=}N{-}O}^{\bullet})(\mathrm{H}) \longrightarrow >\mathrm{Si}^{\bullet}(\mathrm{H}) + \mathrm{N_2O} \text{ (channel 1)}, \tag{VI}$$
$$>\mathrm{Si}(\mathrm{N{=}N{-}O}^{\bullet})(\mathrm{H}) \longrightarrow >\mathrm{Si}^{\bullet}(\mathrm{OH}) + \mathrm{N_2} \text{ (channel 2)}.$$

Only the lower estimate of the rate constant of this reaction of hydrogen atom transfer can be obtained: $k_2(\mathrm{H}, 77\ \mathrm{K}) \gg 10^{-3}\ \mathrm{s^{-1}}$ (which is lower than the reciprocal time of system photolysis (~10^3 s)). If the value of the rate constant of D atom transfer for the deuterated radical is extrapolated to 77 K and we consider that, in the case of the classical isotope effect, the activation energy of the hydrogen atom transfer should be decreased by 1.5 kcal/mol [15], we obtain $k_2(\mathrm{H}, 77\ \mathrm{K}) = 10^{-25}\ \mathrm{s^{-1}}$. This pronounced difference can only be explained by the fact that hydrogen atom transfer in the $>\mathrm{Si}(\mathrm{O}^{\bullet})(\mathrm{H})$ radical occurs via the tunneling mechanism.

2. Thermochemical Method for the Preparation of Oxy Radicals in the Systems $>\mathrm{Si}(\mathrm{O{-}C}^{\bullet}{=}\mathrm{O})(\mathrm{R})$ and $>\mathrm{Si}(\mathrm{N{=}N{-}O}^{\bullet})(\mathrm{R})$

2.1. Thermal decomposition of the $>\mathrm{Si}(\mathrm{O{-}C}^{\bullet}{=}\mathrm{O})(\mathrm{CH_3})$ radical. When the sample containing the $>\mathrm{Si}(\mathrm{O{-}C}^{\bullet}{=}\mathrm{O})(\mathrm{CH_3})$ radicals is allowed to stay at 373 K in a vacuum (under evacuation), oxy radicals decay (this was monitored by a decrease in the intensity of the ESR spectrum) and new product radicals $>\mathrm{Si}^{\bullet}{-}\mathrm{CH_3}$ and $>\mathrm{Si}(\mathrm{CH_2^{\bullet}})(\mathrm{OH})$ are synchronously formed. The ESR spectrum of reaction products is shown in Fig. 4a. The same figure shows individual ESR spectra of the radicals $>\mathrm{Si}^{\bullet}{-}\mathrm{CH_3}$ (Fig. 4b) and $>\mathrm{Si}(\mathrm{CH_2^{\bullet}})(\mathrm{OH})$ (Fig. 4c). In the course of the thermal reaction, the formation of $\mathrm{CO_2}$ and CO was registered by the volumetric method.

The formation of the above products should be associated with the thermal decomposition of oxycarbonyl

Table 2. The rate constants of the reaction $>\mathrm{Si}(\mathrm{O}^{\bullet})(\mathrm{RH}) \longrightarrow >\mathrm{Si}(\mathrm{OH})(\mathrm{R}^{\bullet})$

Radical	k_2, $\mathrm{s^{-1}}$ (E_a^*, kcal/mol)	T, K
$>\mathrm{Si}(\mathrm{O}^{\bullet})(\mathrm{H})$	$(0.1 \pm 0.2) \times 10^5$ (13.5)	373
$>\mathrm{Si}(\mathrm{O}^{\bullet})(\mathrm{CH_3})$	$(2.0 \pm 0.4) \times 10^2$ (17)	373
$>\mathrm{Si}(\mathrm{O}^{\bullet})(\mathrm{C_2H_5})$	$\geq 10^6$ (≤ 10)	373
$>\mathrm{Si}(\mathrm{O}^{\bullet})(\mathrm{CH_3})$	$(0.1 \pm 0.2) \times 10^{-3}$ (18)	250
$>\mathrm{Si}(\mathrm{O}^{\bullet})(\mathrm{D})$	$(2.3 \pm 0.4) \times 10^{-3}$ (15)	210
$>\mathrm{Si}(\mathrm{O}^{\bullet})(\mathrm{CD_3})$	$(0.1 \pm 0.2) \times 10^{-3}$ (18)	250

* Activation energies of processes calculated assuming that $A_0 = 10^{13}\ \mathrm{s^{-1}}$ for the reaction with the participation of the first radical and $A_0 = 10^{12}\ \mathrm{s^{-1}}$ for other reactions.

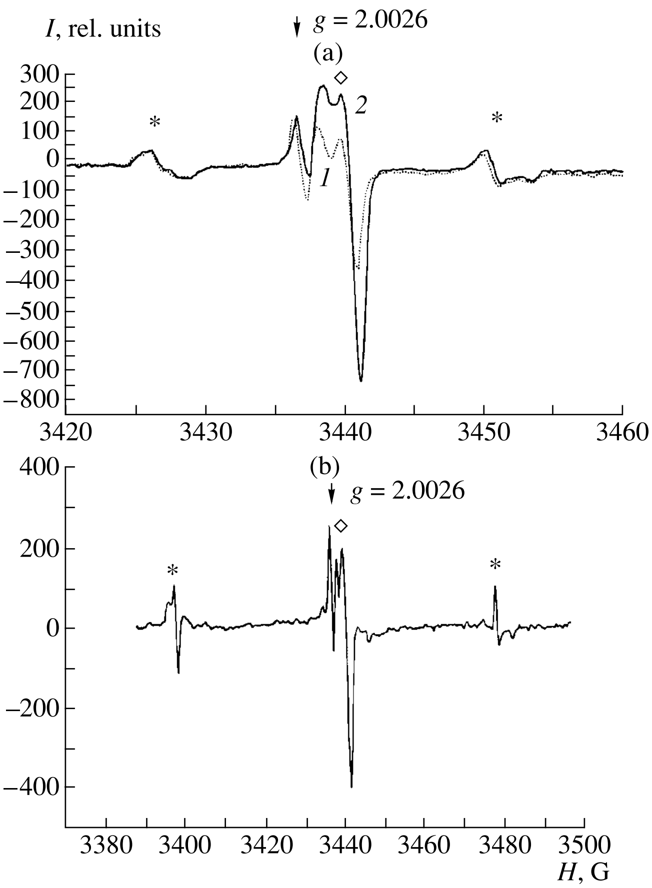

Fig. 3. ESR spectra of photolysis products of radicals $>Si(N{=}N{-}O^{\bullet})(H, D)$ (singlet line with a *g*-factor of 2.0026 belongs to a foreign signal): (a) (*1*) after irradiation of $>Si(N{=}N{-}O^{\bullet})(D)$ at 77 K and (2) after sample heating for 5 min at 230 K (lines marked with a rhomb and a star belong to radicals $>Si^{\bullet}OD$ and $>Si^{\bullet}D$, respectively); (b) after $>Si(N{=}H{-}O^{\bullet})(H)$ irradiation at 77 K (lines marked with a rhomb and a star belong to the $>Si^{\bullet}OH$ and $>Si^{\bullet}H$ radicals, respectively). Recording at 77 K.

radicals via two channels: with the elimination of CO and CO_2:

$$>Si(O{-}C^{\bullet}{=}O)(CH_3) \underset{k_{-1}}{\overset{k_1}{\rightleftarrows}} >Si(O^{\bullet})(CH_3) + CO \xrightarrow{k_2} >Si(CH_2^{\bullet})(OH) + CO, \quad \text{(VII)}$$

$$>Si(O{-}C^{\bullet}{=}O)(CH_3) \underset{k_{-3}}{\overset{k_3}{\rightleftarrows}} >Si^{\bullet}(CH_3) + CO_2. \quad \text{(VIII)}$$

The ratio of yields of radical products is shown in Table 3.

When the thermal decomposition of radicals was carried out in a CO_2 atmosphere ($P_{CO_2} \approx 10^{-1}$ torr, T = 373 K, a reaction time of ~60 min), the only products of the reaction were carbon-centered radicals. Figure 4c shows their ESR spectrum. This channel for the product formation became dominating, because silyl radicals transform into oxycarbonyl radicals in a CO_2 atmosphere via the reverse reaction (reaction VIII).

If the process is carried out in a CO atmosphere ($P_{CO} = 10^{-1}$ torr, T = 373 K), the only product of decomposition is the silyl radical. Figure 4b shows its ESR spectrum. The channel for the formation of the second product under these conditions is completely suppressed because of an equilibrium shift to the left in reaction (VII) in a CO atmosphere.

Thus, by changing the CO pressure on the sample, we can change the ratio of product yields and obtain information on the rate constant k_2.

Using the method of steady-state concentrations for the $>Si(O^{\bullet})(CH_3)$ radicals, we derived the following expression for the ratio of the product yields depending on CO pressure:

$$[>Si^{\bullet}CH_3]/[>Si(CH_2^{\bullet})(OH)] = k_3(k_{-1}P_{CO} + k_2)/(k_1k_2). \quad (1)$$

At $P_{CO} = 0$, we obtain $k_3/k_1 = 1.25$. At $P_{CO} = (1.5 \pm 0.4) \times 10^{-4}$ torr (373 K), the ratio of product yields was equal to unity (see Table 3). Therefore, we obtain from formula (1) that $k_{-1}P_{CO} \approx k_2$(373 K). If the value of k_{-1} is set to 1.6×10^{-12} cm^3 molecule^{-1} s^{-1} (for reaction $HO^{\bullet} + CO \longrightarrow H{-}O{-}C^{\bullet}{=}O$ [16]), we obtain k_2 (373 K) ≈ 2×10^2 s^{-1} (see Table 2).

The value of k_2 for this reaction at 250 K was measured earlier (see subsection 1.1): $k_2(250\ K) = (1.0 \pm 0.2) \times 10^{-3}$ s^{-1}. Assuming that the dependence of k_2 on temperature is of Arrhenius type, we obtain $k_2 = 6 \times 10^{12}\exp(-(18\ kcal/mol)/RT)$. Note that the value of the preexponential factor is reasonable in this expression.

2.2. Thermal decomposition of the $>Si(O{-}C^{\bullet}{=}O)(CH_2{-}CH_3)$ radical. It was found in [5] that, if the sample containing the $>Si(O{-}C^{\bullet}{=}O)(CH_2{-}CH_3)$ radical is allowed to stay for a long time at 300 K, the equilibrium is established between the radicals

$>Si(O{-}C^{\bullet}{=}O)(CH_2{-}CH_3)$ (**A**),

$>Si(O{-}CH{=}O)(CH_2{-}CH_2^{\bullet})$ (**B**),

$>Si(O{-}CH{=}O)(CH^{\bullet}{-}CH_3)$ (**C**).

When this system is heated to 373 K in a vacuum (under evacuation), the ESR method registered the decay of radicals **A**, **B**, and **C** and the simultaneous appearance of radicals $>Si(OH)(CH_2{-}CH_2^{\bullet})$ and $>Si^{\bullet}{-}CH_2{-}CH_3$ (the ratio of their concentrations is shown in Table 3). Based on these experimental data the scheme of the process of thermal decomposition of rad-

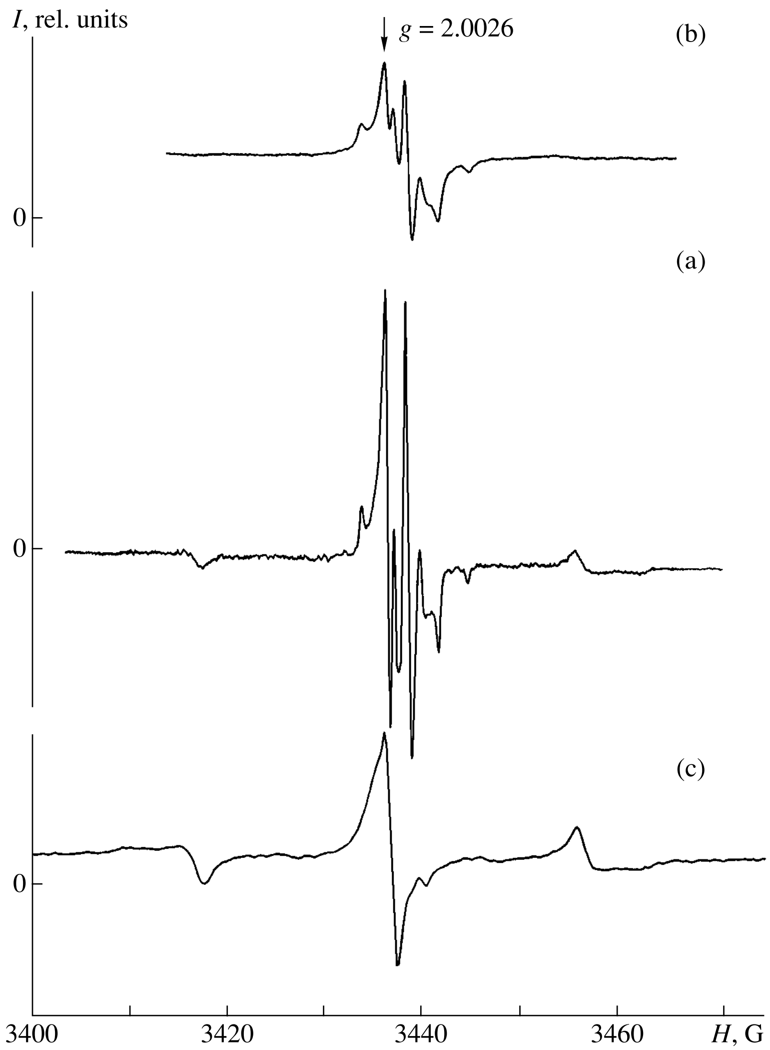

Fig. 4. ESR spectra of (a) products of thermal decomposition of (T = 373 K) the $>\mathrm{Si(O{-}C^{\bullet}{=}O)(CH_3)}$ radicals and the superposition of ESR spectra of radicals $>\mathrm{Si^{\bullet}{-}CH_3}$ and $>\mathrm{Si(CH_2^{\bullet})(OH)}$; (b) $>\mathrm{Si^{\bullet}{-}CH_3}$ radicals; and (c) $\mathrm{Si(CH_2^{\bullet})(OH)}$ radicals. Recording at 77 K.

icals in this system in a vacuum can be described as follows:

$$>\mathrm{Si(O{-}CH{=}O)(CH^{\bullet}{-}CH_3)}$$

$$\longleftrightarrow\ >\mathrm{Si(O{-}C^{\bullet}{=}O)(CH_2{-}CH_3)}$$

$$\longrightarrow\ >\mathrm{Si(O^{\bullet})(CH_2{-}CH_3)} + \mathrm{CO}$$

$$\longrightarrow\ >\mathrm{Si(OH)(CH_2{-}CH_2^{\bullet})} + \mathrm{CO},$$

$$>\mathrm{Si(O{-}C^{\bullet}{=}O)(CH_2{-}CH_3)}$$

$$\longrightarrow\ >\mathrm{Si^{\bullet}(CH_2{-}CH_3)} + \mathrm{CO_2}.$$

The results of IR spectroscopic measurements support this mechanism of thermal decomposition of radicals. Figure 5 shows the difference IR spectrum of the sample after its heating at 373 K. We see the disappearance of the bands at 2945 and 2975 cm^{-1}, which refer to the stretching vibrations of the C–H bonds in the $>\mathrm{Si(O{-}CH{=}O)(CH^{\bullet}{-}CH_3)}$ radical, and the appearance of three new bands at 3739, 3119, and 3032 cm^{-1}. The band at 3739 cm^{-1} is due to the stretching vibrations of the O–H bond in the Si–O–H group. This is characteristic of the Si–O–H group that has a hydrocarbon substituent at the silicon atom [17] (for the terminal $\mathrm{({\equiv}Si{-}O)_3Si{-}O{-}H}$ group on the silica surface, the frequency is 3749 cm^{-1}). The bands at 3119 and 3032 cm^{-1} should be assigned on the basis of literature data [18] to the antisymmetric and symmetric vibrations of C–H bonds in the terminal CH$_2$ group of the hydrocarbon radical $\mathrm{R{-}CH_2{-}CH_2^{\bullet}}$ Thus, these IR spectroscopic data support the conclusion that the $>\mathrm{Si(OH)(CH_2{-}CH_2^{\bullet})}$

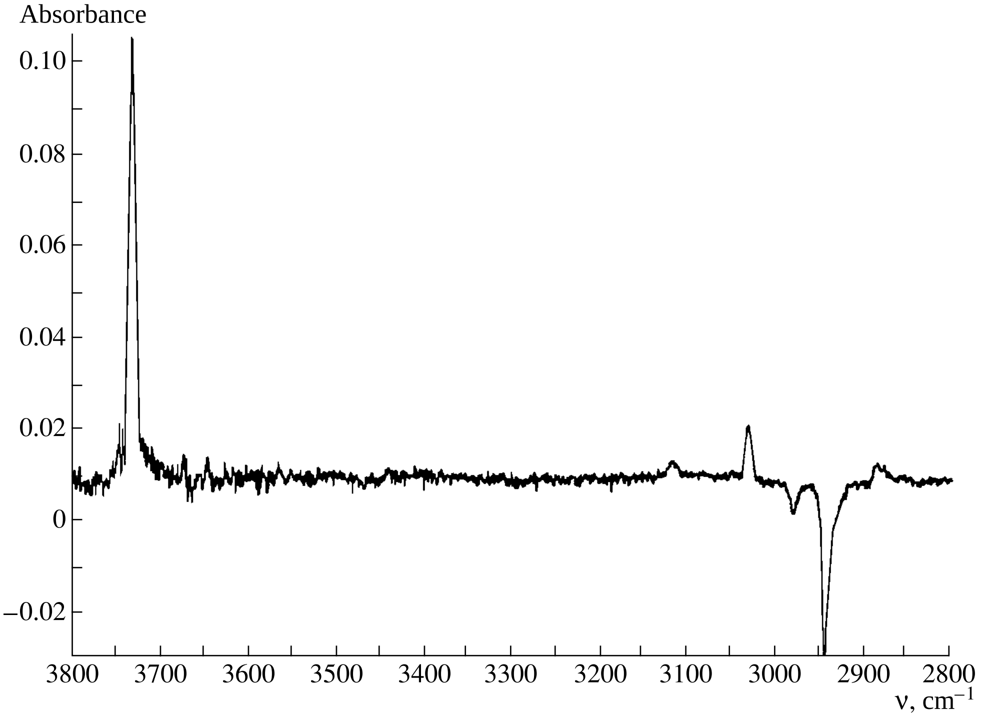

Fig. 5. Difference IR spectrum (difference of bands measured before and after the reaction) for the process of radical transformation $>Si(O–CH=O)(CH^{\bullet}–CH_3) \longrightarrow >Si(OH)(CH_2–CH_2^{\bullet})$ (heating at 373 K).

radical is formed in the course of the reaction. The formation of the only product is associated with the conditions of this experiment. We did not remove volatile decomposition products (CO and CO_2). As a result, the main portion of the products consisted of $>Si(OH)(CH_2–CH_2^{\bullet})$ radicals. In a CO_2 atmosphere, the $>Si^{\bullet}–CH_2–CH_3$ radicals transform into $>Si(OH)(CH_2–CH_2^{\bullet})$: $>Si^{\bullet}(CH_2–CH_3) + CO_2 \longrightarrow >Si(O–C^{\bullet}=O)(CH_2–CH_3) \longrightarrow >Si(OH)(CH_2–CH_2^{\bullet}) + CO$.

Table 3. Ratio of yields (W) of products of thermal decomposition of radicals ($T = 373$ K)

Radical	P_{CO}, torr	W
$W = [>Si(OH)(R^{\bullet})]/[>Si^{\bullet}(RH)]$		
$>Si(O–C^{\bullet}=O)(CH_3)$	Vacuum	0.8
	$(1.5 \pm 0.4) \times 10^{-4}$	1
$>Si(O–C^{\bullet}=O)(CH_2–CH_3)$	Vacuum	2.6
	30 ± 0.5	2.6
$W = [>Si^{\bullet}(OH)]/[>Si^{\bullet}H]$		
$>Si(O–C^{\bullet}=O)(H)$	Vacuum	5.7
	(1.2 ± 0.2)	1
$>Si(N=N–O^{\bullet})(H)$	Vacuum	100
	(1.0 ± 0.2)	1

Note that the oxy radical formed in the elimination of CO abstracts a hydrogen atom from the CH_3 group of the $–CH_2–CH_3$ fragment rather than from the CH_2-group, although the latter channel is thermodynamically more favorable. This points to the fact that the main factor here is a decrease in the activation energy of hydrogen abstraction when passing from the four-membered transition state to a five-membered one.

We failed to measure the rate constant k_2 in this system. An increase in the CO pressure in the system to 30 torr ($T = 373$ K) did not result in a change in the ratio of radical product yields. Thus, we were only able to obtain a lower estimate of the constant: $k_2 \geq 10^6$ s^{-1} ($E_a \leq$ 10 kcal/mol) (see Table 2).

Earlier, the thermal decomposition of the $(\equiv Si–O)_3Si–O–C^{\bullet}=O$ radicals was studied [10] and it was found that the main channel is the elimination of the CO_2 molecule and the formation of the silyl radical $(\equiv Si–O)_3Si^{\bullet}$. At the same time, the study of the products from the thermal decomposition of radicals

$(\equiv Si{-}O)_2Si(O{-}C^{\bullet}{=}O)(R)$ (R = H (see sections 2 and 3), CH_3, C_2H_5) shows that their thermal decomposition occurs via two channels with comparable yields: via the elimination of CO_2 and CO. Thus, a change in the chemical nature of one of the substituents at a silicon atom resulted in a substantial increase in the role of the second channel for the radical center transformation.

2.3. Thermal transformations of radicals $>Si(O{-}C^{\bullet}{=}O)(H)$ and $>Si(N{=}N{-}O^{\bullet})(H)$. The formation of products of two main types was also registered in the thermal decomposition (T = 373 K, vacuum) of $>Si(O{-}C^{\bullet}{=}O)(H)$ radicals (see Table 3):

$$>Si(O{-}C^{\bullet}{=}O)(H) \longrightarrow >Si^{\bullet}(H) + CO_2,$$

$$>Si(O{-}C^{\bullet}{=}O)(H) \longrightarrow >Si^{\bullet}(OH) + CO.$$

In a CO atmosphere (P_{CO} = 1.2 torr, T = 373 K), the ratio of product yields changed (see Table 3). This allowed us to determine the rate constant k_2 (373 K) for this process using formula (1) (Table 2).

Heating the radical $>Si(N{=}N{-}O^{\bullet})(H)$ at 373 K led to its decomposition, the quantitative formation of molecular nitrogen (according to the results of volumetric measurements), and the appearance of the new paramagnetic center, which is the $>Si^{\bullet}(OH)$ radical (Fig. 6). Moreover, we registered the formation of nitrous oxide elimination products in small amounts (~1%).

To determine the rate constant k_2, the thermal decomposition of the $>Si(N{=}N{-}O^{\bullet})(H)$ radicals was carried out in a CO atmosphere. In this case, as well as in the experiment with the oxycarbonyl radical, we registered two products using ESR spectroscopy: $>Si^{\bullet}(OH)$ and $>Si^{\bullet}H$ radicals (their yields are shown in Table 3). The value of the rate constant is shown in Table 2.

If we assume that the transfer of a hydrogen atom at 373 K in the $>Si(O^{\bullet})(H)$ radical occurs with the usual overcoming of an activation barrier, then its height is E_a = 13.5 kcal/mol (if we assume the preexponential factor equal to 10^{13} s^{-1}). This value agrees well with the height of the activation barrier estimated from the data on D transfer in this system (the 1.5-kcal/mol difference can be associated with the difference in the zero-point energies of atoms H and D [15]). Therefore, the reaction of hydrogen atom transfer at 373 K occurs via the classical over-the-barrier pathway.

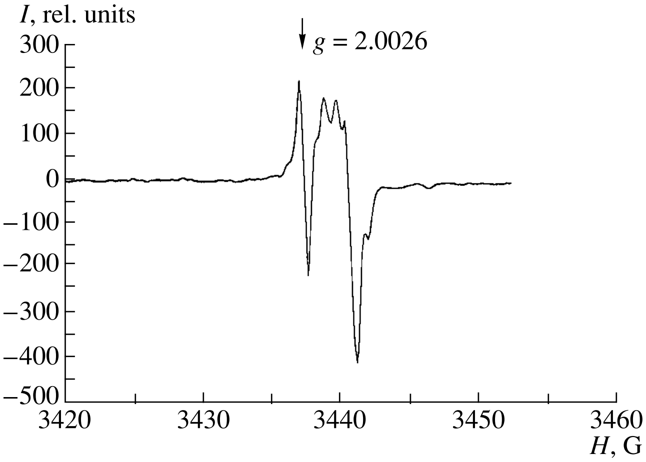

Fig. 6. ESR spectrum of radicals $>Si^{\bullet}(OH)$, which is the product of thermal decomposition at 373 K of the radicals $>Si(N{=}N{-}O^{\bullet})(H)$ (the singlet line with a g-factor of 2.0026 belonging to the foreign signal). Recording at 295 K.

It was shown in subsection 1.2 that the reaction of hydrogen atom transfer to the oxy radical in the $>Si(O^{\bullet})(H)$ system at 77 K occurs at a high rate, and we hypothesized that this is stipulated by tunneling of the hydrogen atom under these conditions. Thus, with a decrease in temperature the mechanism of hydrogen atom transfer changes in this system.

A temperature at which the rates of over-the-barrier pathway and under-the-barrier tunneling of the atom (usually, these are light H or D atoms) are equal is called the critical temperature T_{cr} [19]. The rate constant of tunneling can be described in the simplest case in the following form: $k_{tunnel} = \nu_0 \exp\left(-\frac{2}{h}\int(2mE(x))^{0.5}dx\right) = \nu_0\exp(-\alpha)$, where ν_0 is the frequency of collisions of the tunneling atom and a barrier (~10^{13} s^{-1} for H and D atoms), m is the weight of the tunneling atom, and $E(x)$ is the potential energy surface of the system [19]. In the case of the classical over-the-barrier pathway, the temperature dependence of the reaction rate constant has the Arrhenius form: $k_A = \nu_0\exp(-E_a/RT)$. Therefore, the critical temperature is determined by the following expression:

$$T_{cr} = E_a/(R\alpha). \qquad (2)$$

The obtained experimental data make it possible to estimate the interval of possible values of α. Indeed, in the case of the D-containing radical, the value of the critical temperature is lower than 150 K (see Fig. 2). Therefore, $\alpha(D) \ge E_a/(RT_{cr}) \cong 15\,000/300 = 50$. Because $\alpha \sim m^{0.5}$, it should be expected on switching from D to H that $\alpha(H) \ge 35$. On the other hand, the rate constant of the tunneling hydrogen atom transfer at 77 K $k_{tunnel} = \nu_0\exp(-\alpha) \ge 10^{-2}$ s^{-1}. Therefore, assuming $\nu_0 = 10^{13}$ s^{-1}, we obtain that $\alpha(H) \le 34.5$. Thus, the experimental data

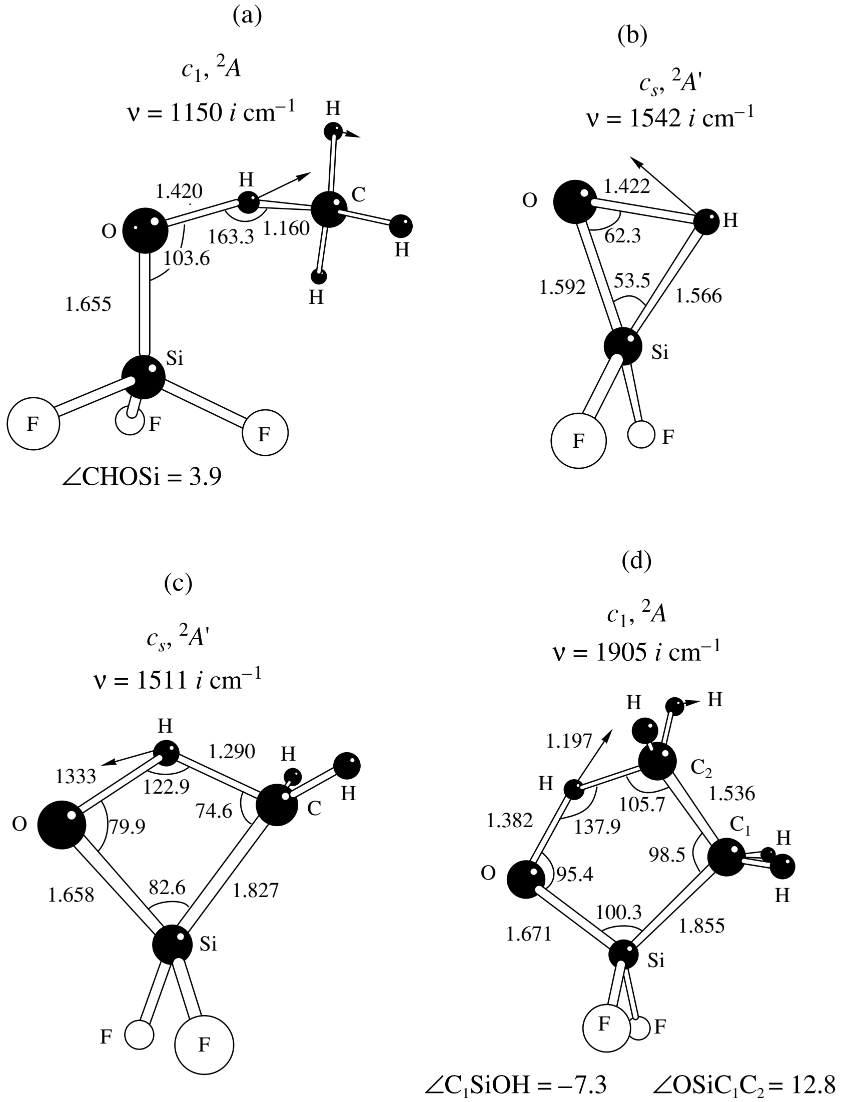

Fig. 7. Structures of transition states for the reactions of hydrogen atom transfer, their symmetry, and the calculated minimal frequency of motion along the reaction coordinate (ν). Points refer to the directions of atom shifts in the transition states of reactions (a) $F_3Si{-}O^{\bullet} + HCH_3 \longrightarrow F_3Si{-}O{-}H + {}^{\bullet}CH_3$, (b) $F_2Si(H)(O^{\bullet}) \longrightarrow F_2Si^{\bullet}(OH)$, (c) $F_2Si(CH_3)(O^{\bullet}) \longrightarrow F_2Si(CH_2^{\bullet})(OH)$, and (d) $F_2Si(C_2H_5)(O^{\bullet}) \longrightarrow F_2Si(CH_2{-}CH_2^{\bullet})(OH)$.

suggest that the value α(H) of the process under consideration is ~35 and the critical temperature for the H atom transfer is ~200 K according to formula (2). The results of measurements of the rate constant of this reaction at 373 K are in agreement with the above estimate. These results suggest that the hydrogen atom transfer occurs via the classical, over-the-barrier pathway under these conditions.

Thus, we obtained experimental data on the rate constants of H(D) atom transfer in the $>Si(O^{\bullet})(R)$ radicals, where R = H, CH_3, and C_2H_5. Based on these data, we estimated the activation energies of the corresponding reactions: 13.5 ± 1, 18 ± 1, <10 kcal/mol, respectively. The considered reactions demonstrate the dependence of the activation energy on the size of the cyclic transition state. The most unfavorable is the four-membered rather than three-membered transition state. Radicals of the $\equiv Si{-}O^{\bullet}$ type are very reactive in the reactions of hydrogen atom abstraction from saturated hydrocarbons [4]. According to these data, the activation energy of the reaction of oxy radical with the methane molecule is at most 1–2 kcal/mol (in this case, the transition state is not cyclic). Thus, the high activation energies of hydrogen atom transfer in the $>Si(O^{\bullet})(R)$ radicals are stipulated by the structures of the corresponding transition states, in which the radical center and the hydrogen atom approach each other as a result of the substantial deformation of the initial structure.

3. Quantum-Chemical Modeling of Hydrogen Atom Transfer with the Participation of Oxy Radicals

Figure 7 shows the structures of transition states (TS) for reactions with the participation of radicals that model surface sites (the choice of this models was justified in [20]). Along with cyclic transition states, we also calculated a linear transition state for hydrogen abstraction by the oxy radical from the methane molecule. These data give an idea of the degree of deformation in the transition state geometries.

Below we provide the results of calculations of hydrogen transfer energetics (enthalpies and activation energies in kcal/mol at 0 K) in various systems. Calculations were carried out using density functional theory (DFT) in the UB3LYP/6-311G** variant [22, 23]). For most of the structures, calculations at a higher level G2MP2//UB3LYP/6-311G** were also carried out. This is one of the variants of the calculation scheme G2 [21], in which geometries and vibrational spectra were determined using the DFT method. The G2 methods were specially developed for thermochemical calculations. These results are presented in parentheses (in kcal/mol):

$$F_3Si{-}O^{\bullet} + HCH_3 \longrightarrow TS + 0.5 \longrightarrow F_3Si{-}O{-}H + {}^{\bullet}CH_3 \qquad -19.3(-23.4),$$

$$F_2Si(H)(O^{\bullet}) \longrightarrow TS + 20.3(17.1) \longrightarrow F_2Si^{\bullet}(OH) \qquad -21.6(-26.1),$$

$$F_2Si(CH_3)(O^{\bullet}) \longrightarrow TS + 22.9(22.4) \longrightarrow F_2Si(CH_2^{\bullet})(OH) \qquad -18.3(-22.4),$$

$$F_2Si(C_2H_5)(O^{\bullet}) \longrightarrow TS + 11.6 \longrightarrow F_2Si(CH_2{-}CH_2^{\bullet})(OH) \qquad -19.1.$$

The reaction enthalpy was calculated by extrapolating the reaction enthalpies for smaller systems calculated at the G2 level to the latter reaction. This gives us a value of –23 kcal/mol.

First, we would like to note that, for the reaction of hydrogen atom abstraction by the oxysilyl radical from the methane molecule, the calculation predicts an activation energy close to zero, which agrees with the experimental data [8]. Note also that the enthalpies of hydrogen atom transfer reactions with the participation of oxysilyl radicals are higher than 20 kcal/mol, which is higher than for the analogous reactions with the participation of their hydrocarbon analogs, $H_3C{-}O^{\bullet}$. According to the published data, the enthalpy of reaction $H_3C{-}O^{\bullet} + HCH_3 \longrightarrow H_3C{-}O{-}H + {}^{\bullet}CH_3$ is 0.8 kcal/mol [24]. This is due to the high strength of the O–H-bond in the silanone group.

Calculations predict a trend in the changes of the activation energies in the considered series of reactions that agree with experimental data. The maximal activation energy was calculated for the reaction of hydrogen atom transfer in the $F_2Si(CH_3)(O^{\bullet})$ radical with a cyclic transition state.

ACKNOWLEDGMENTS

The experimental part of this work was carried out with the participation of S.N. Dubrovina. This work was supported by the Russian Foundation for Basic Research (grant no. 00-03-32069). Quantum-chemical calculations were carried out using Gaussian-94 [13] at the institute of Organic Chemistry, Russian Academy of Sciences (Russian Foundation for Basic Research grant no. 98-07-90290).

REFERENCES

1. Radtsig, V.A., *Kinet. Katal.*, 1983, vol. 24, no. 1, p. 173.
2. Radtsig, V.A., *Khim. Fiz.*, 1995, vol. 14, no. 8, p. 125.
3. Radtsig, V.A. and Kostritsa, S.N., *Izv. Akad. Nauk, Ser. Khim.*, 1997, no. 8, p. 1468.
4. Bobyshev, A.A. and Radtsig, V.A., *Kinet. Katal.*, 1990, vol. 31, no. 4, p. 925.
5. Radtsig, V.A., *Kinet. Katal.*, 2002, vol. 43, no. 4, p. 526.
6. Morterra, C. and Low, M.J.D., *Ann. N. Y. Acad. Sci.*, 1973, vol. 220, p. 135.
7. Radzig, V.A., *Colloids Surf., A: Physicochem. Eng. Aspects.*, 1993, vol. 74, p. 91.
8. Radtsig, V.A., *Kinet. Katal.*, 1996, vol. 37, no. 2, p. 302.
9. Radtsig, V.A., *Kinet. Katal.*, 1999, vol. 40, no. 5, p. 764.
10. Radtsig, V.A. and Bystrikov, A.V., *Kinet. Katal.*, 1978, vol. 19, no. 3, p. 713.
11. Radtsig, V.A., *Kinet. Katal.*, 2001, vol. 42, no. 5, p. 696.
12. Bagratashvili, V.N., Tsypina, S.I., Radtsig, V.A., *et al.*, *J. Non-Cryst. Solids*, 1995, vol. 180, p. 221.
13. Gaussian 94, Revision D. 1. Frisch, M.J., Trucks, G.W., Schlegel, H.B., Gill, P.M.W., Johnson, B.G., Robb, M.A., Cheeseman, J.R., Keith, T., Petersson, G.A., Montgomery, J.A., Raghavachari, K., Al-Laham, M.A., Zakrzewski, V.G., Ortiz, J.V., Foresman, J.B., Cioslowski, J., Stefanov, B.B., Nanayakkara, A., Challacombe, M., Peng, C.Y., Ayala, P.Y., Chen, W., Wong, M.W., Andres, J.L., Replogle, E.S., Gomperts, R., Martin, R.L., Fox, D.J., Binkley, J.S., Defrees, D.J., Baker, J., Stewart, J.P., Head-Gordon, M., Gonzalez, C., and Pople, J.A., *Pittsburgh PA*, Gaussian, Inc, 1995.

14. Bobyshev, A.A. and Radtsig, V.A., *Kinet. Katal.*, 1988, vol. 29, no. 3, p. 638.
15. Emmanuel, N.M. and Knorre, D.G., *Kurs khimicheskoi kinetiki* (Chemical Kinetics), Moscow: Vysshaya Shkola, 1962, p. 414.
16. Larson, C.W., Stewart, P.H., and Golden, D.M., *Int. J. Chem.*, 1988, vol. 20, p. 27.
17. Radtsig, V.A. and Kostritsa, S.N., *Kinet. Katal.*, 2000, vol. 41, no. 2, p. 267.
18. Pakansky, J., Brown, D.W., and Chang, J.S., *J. Phys. Chem.*, 1981, vol. 85, no. 17, p. 2562.
19. Gol'danskii, V.I., *Dokl. Akad. Nauk SSSR*, 1959, vol. 124, p. 1261.
20. Radtsig, V.A., *Khim. Fiz.*, 2000, vol. 19, no. 3, p. 17.
21. Curtiss, L.A., Raghavachari, K., and Pople, J.A., *J. Chem. Phys.*, 1993, vol. 98, no. 2, p. 1293.
22. Becke, A.D., *J. Chem. Phys.*, 1993, vol. 98, no. 7, p. 5648.
23. Lee, C., Yang, W., and Parr, R.G., *Phys. Rev. B*, 1988, vol. 37, no. 2, p. 785.
24. Chase, M.W., Davies, C.A., Downey, J.R., and Frurip, D.J., *J. Phys. Chem. Ref. Data*, 1985, Suppl. 1, vol. 14, p. 1.